Assimilated inversion of NO_x emissions over east Asia using OMI NO_2 column measurements

Chun Zhao[1] and Yuhang Wang[1]

[1] Assimilated inversion on a daily basis using OMI tropospheric NO_2 columns is developed and applied in a regional chemical transport model (REAM) to constrain fossil fuel (FF) NO_x emissions over east Asia in 2007. The iterative nature of the assimilated inversion improves upon the widely used monthly-mean inversion by accounting for the chemical feedbacks of changed NO_x emissions and reducing the dependence of the a priori emissions. The assimilated a posteriori emissions from FF combustion over east Asia are 9.5 Tg N/yr comparable to 10.9 Tg N/yr of the a priori. Significant changes in the spatial distribution of FF NO_x emissions are found in the assimilated inversion from the a priori or monthly-mean inversion. The assimilated inversion shows that the a priori FF NO_x emission inventory tends to overestimate the emissions over the economically developed areas and underestimate over the underdeveloped areas in East China, which may reflect in part FF NO_x emission reductions resulting from the urban-centric air quality controls in China. **Citation:** Zhao, C., and Y. Wang (2009), Assimilated inversion of NO_x emissions over east Asia using OMI NO_2 column measurements, *Geophys. Res. Lett.*, *36*, L06805, doi:10.1029/2008GL037123.

1. Introduction

[2] Ozone (O_3) is a key pollutant, a greenhouse gas, and an important factor in determining the oxidizing power of the atmosphere. It is largely controlled by nitrogen oxides (NO_x = NO + NO_2) in the troposphere. NO_x in the troposphere originates from fossil fuel combustion, lightning and soils. The traditional bottom-up approach to estimate NO_x emissions makes use of compilations of emission statistics and source factors. For fossil fuel sources, for example, emission factors are generally developed for industry, domestic, transport and power plants. In regions such as China, where emission statistics and characteristics are incomplete, the bottom-up inventory uncertainties could be large [e.g., *Streets et al.*, 2003]. Global tropospheric NO_2 distributions were measured by several satellite instruments in the last decade. Many studies showed that satellite measurements provide important top-down constraints for improving emission inventories [e.g., *Martin et al.*, 2003, 2006; *Wang et al.*, 2007b; *Choi et al.*, 2008a].

[3] China contributes significantly to the global NO_x budget, and its NO_x emission inventories based on the bottom-up approach are thought to be quite uncertain [e.g., *Streets et al.*, 2003; *Zhang et al.*, 2007]. *Ma et al.* [2006]

compared NO_2 columns inferred from GOME over China with model results using three different bottom-up inventories of NO_x. They found that the model underestimated the GOME observations for China with a negative bias of 31% -67%. *Wang et al.* [2007b] found a low model bias of 40% with anthropogenic NO_x emissions taken from the Global Emission Inventory Activity (GEIA) [*Benkovitz et al.*, 1996] for East China. They developed a top-down inventory of surface NO_x emissions for East China using GOME measurements for a 3-year period (1997, 1998, and 2000), and found that the a posteriori estimate of fuel combustion NO_x emissions for East China is 3.72 Tg N/yr, 15% higher than the a priori. A large underestimation of soil NO_x emissions was suggested by their study.

[4] Due in part to the poor temporal resolutions available from GOME and SCIAMACHY satellite measurements, all previous applications of the top-down approach in optimizing NO_x emissions were on a monthly-mean basis [e.g., *Martin et al.*, 2003; *Wang et al.*, 2007b; *Boersma et al.*, 2008]. The improvement in temporal and spatial resolutions of the recent OMI instrument [*Boersma et al.*, 2007] provides an opportunity to apply an assimilated inversion on a daily basis to derive an optimized NO_x inventory, which allows for iterative adjustments of the NO_x emissions compared to one single inversion in the previously used monthly-mean approach. One important benefit of the daily assimilated inversion is that chemical feedbacks driven by changing NO_x emissions, such as the nonlinear feedback through OH [*Stavrakou et al.*, 2008], are taken into account.

[5] We develop and implement the daily assimilated inversion into a 3-D chemical transport model to derive optimized surface NO_x emissions over east Asia ($80-150°E$, $10-50°N$) with the OMI NO_2 measurements in July 2007. The method is not meant to constrain the day-to-day variation of NO_x emissions. The a posteriori NO_x emissions from the daily assimilated inversion are compared with those from a priori inventories and monthly-mean inversions to demonstrate the advantages of the assimilated inversion. Two a priori emission inventories are used to investigate the sensitivity of the inversion results to the a priori inventory. Lastly, we derive the a posteriori fossil fuel NO_x emissions in the region. The a priori and monthly-mean and daily assimilated a posteriori emissions are evaluated using OMI measurements in August 2007.

2. OMI Tropospheric NO_2 Columns

[6] OMI onboard the NASA Aura satellite has a daily global coverage, and passes cross the equator at 1:45 PM local time. The nadir horizontal resolution of OMI is 24 × 13 km^2. The retrieved tropospheric NO_2 columns and its uncertainties are available from two independent products:

[1]School of Earth and Atmospheric Science, Georgia Institute of Technology, Atlanta, Georgia, USA.

near-real time (NRT) tropospheric NO$_2$ columns retrieved by KNMI/NASA [*Boersma et al.*, 2007] and OMI standard product at NASA Goddard Earth Sciences Data and Information Services Center (GES-DISC) [*Bucsela et al.*, 2006]. *Bucsela et al.* [2008] found significant difference between the two products. *Lamsal et al.* [2008] found a seasonal component to the bias in the annual mean in the standard product over North America. Our analysis shows that the difference between the NRT product and the standard product is much less over east Asia than over North America in the summer of 2007. The reason is unclear. Therefore, we obtain the ''best-estimates'' of tropospheric NO$_2$ columns by averaging the columns from KNMI and GES-DISC weighted by their uncertainties. We did not attempt to re-calculate the air mass factors in either product. We use two methods to estimate the errors in the combined OMI columns. The first method is to estimate the errors as the root mean square of the uncertainties of the two retrievals. The second method is to estimate the error as the deviations of KNMI and GES-DISC retrievals from their means. We take the larger of the two estimates as the uncertainty for the combined OMI columns, which is around 40% over the polluted regions and reaches a factor of 1.5 over the ocean and clean continent such as western China. Only the OMI tropospheric NO$_2$ column data with cloud fractions of < 30% are used in the study.

3. REAM Model

[7] The REAM model driven by MM5 assimilated meteorological fields (using the NCEP reanalysis) is described by *Choi et al.* [2008a]. In this study, we use WRF in place of MM5, as we found REAM performance better with meteorological fields from WRF compared with satellites and in-situ measurements [*Zhao et al.*, 2008]. Previously, this model was applied to investigate a number of tropospheric chemistry and transport problems at northern mid-latitudes [*Choi et al.*, 2005, 2008a, 2008b; *Jing et al.*, 2006; *Wang et al.*, 2006; *Guillas et al.*, 2008] and in the polar regions [*Zeng et al.*, 2003, 2006; *Wang et al.*, 2007a]. The REAM model has a horizontal resolution of 70 km with 23 vertical layers below 10 hPa. The time steps for transport and chemistry are 5 minutes and 1 hour respectively. Most meteorological inputs in REAM are updated every 30 minutes except those related to convective transport, which are updated every 2.5 minutes. The horizontal domain of WRF has 5 extra grids beyond that of REAM on each side to minimize potential transport anomalies near the boundary. Initial and boundary conditions for chemical tracers in REAM are obtained from the global simulation for 2007 using the GEOS-CHEM model with assimilated meteorology (GEOS5) [*Bey et al.*, 2001]. We ran the daily inversion for July 2007 to obtain the a posteriori emissions. Biogenic emission algorithms are adapted from the GEOS-CHEM model. The lightning NO$_x$ emission is parameterized as *Choi et al.* [2008b]. The anthropogenic emissions of tracers other than NO$_x$ are taken from a recent bottom-up Asian emission inventory developed by D. G. Streets et al. for 2006 INTEX-B campaign (the detail can be obtained from http://www.cgrer.uiowa.edu/EMISSION_DATA_new/index_16.html; hereinafter referred to as Streets2006).

[8] NO$_x$ emissions from fossil fuel combustion are adopted from two recent independent inventories in order to investigate the effect of the a priori inventory on the inversion of NO$_x$ emissions over east Asia. The inventories are Streets2006 and POET2000 prepared by *Granier et al.* [2005] for 2000 with a global coverage, respectively. The emissions over China from both inventories are scaled to 2007 with an annual increasing rate of 8%, which was also used in developing Streets2006 inventory (D. D. Streets, personal communication, 2008). Other studies have found an increase rate of 5–10% [e.g., *Stavrakou et al.*, 2008]. In this manner, we obtain scaled-Streets 2007 and scaled-POET 2007 inventories. The algorithm of soil NO$_x$ emissions follows *Yienger and Levy* [1995] as adopted by *Wang et al.* [1998]. Few fires are observed by the Moderate Resolution Imaging Spectroradiometer (MODIS) [*Kaufman et al.*,1998] over east Asia in July 2007, and *Wang et al.* [2007b] suggested that the biomass burning source is a small portion of the total NO$_x$ emissions over East China. Biomass burning NO$_x$ is therefore excluded in the study.

[9] We estimate the uncertainty of the a priori fossil-fuel combustion inventory as the difference between the scaled-Streets 2007 and scaled-POET 2007 inventories. The uncertainty of soil emissions is estimated as 300% since *Wang et al.* [2007b] concluded that the a priori soil emissions should be increased by a factor of 3 in summer over East China. The overall uncertainty of the a priori surface NO$_x$ emissions is around 60% over most east Asia regions, but reaches 300% over the regions where the soil emissions dominate.

4. Results and Discussion
4.1. A Priori Surface NO$_x$ Emissions and Corresponding Tropospheric NO$_2$ Columns

[10] Model simulations are conducted using either the scaled-Streets 2007 or scaled-POET 2007 inventory (hereafter referred to as case A or case B, respectively). The total a priori surface NO$_x$ emissions over east Asia are 11.6 and 11.1 Tg N/yr in cases A and B, respectively. The fossil fuel source accounts for > 90% of the totals. The distribution of the a priori surface NO$_x$ emissions in case A is shown in Figure 1a. While the total emission amount is similar, the spatial correlation between these two inventories is moderate ($R^2 = 0.4$).

[11] Figure 1b shows observed and simulated monthly mean tropospheric NO$_2$ columns over east Asia for July 2007. The model simulations show large NO$_2$ columns over East China, South Korea and Japan as observed. The difference between model simulations reflects the difference in fossil fuel combustion sources in cases A and B. It is clear that simulated spatial distributions over East China in both cases differ from the OMI measurements.

4.2. A Posteriori Surface NO$_x$ Emissions

[12] We first apply previously used monthly-mean inversion method to estimate the top-down NO$_x$ emission inventory by scaling the a priori emissions with the ratio of observed and simulated tropospheric NO$_2$ column in each grid box. The a posteriori emissions are then estimated as error weighted averages of the a priori and top-down emissions [e.g., *Martin et al.*, 2003, 2006; *Wang et al.*, 2007b]. The uncertainty of the top-down emissions originates from
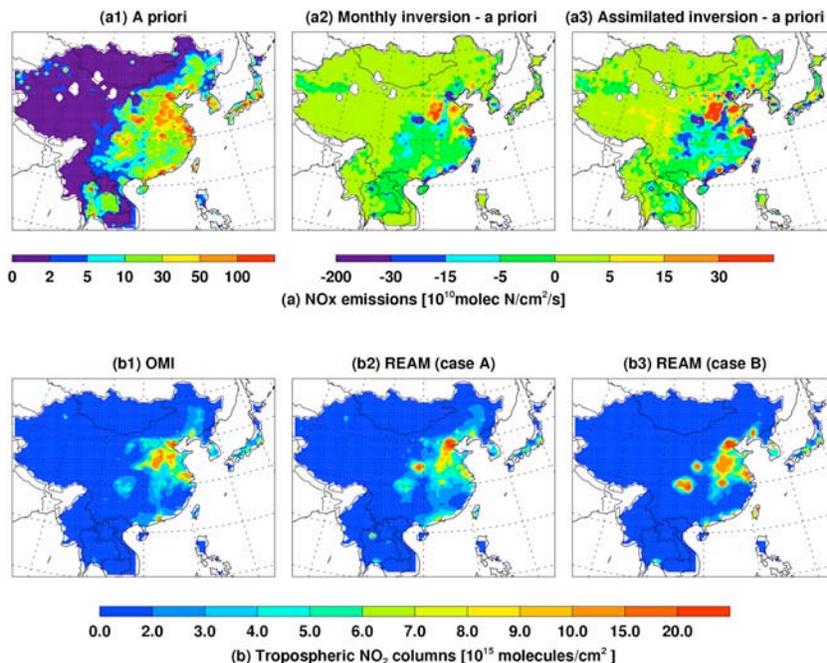
Figure 1. (a) A priori surface NO$_x$ emissions for July 2007 in case A, and the corresponding changes in the a posteriori emissions from the a priori in the monthly and assimilated daily inversions. (b) Monthly mean tropospheric NO$_2$ columns over east Asia for July 2007 from OMI measurements, and the corresponding REAM results with a priori NO$_x$ emissions in case A and case B. Only OMI data with cloud fractions of < 30% are used.

the retrieval error (section 2) and the error of linking local NO$_2$ columns to local emissions on the basis of model simulations. The latter is estimated at 30% from *Martin et al.* [2003]. We compared the model simulated tropospheric NO$_2$ columns using either WRF or MM5 assimilated meteorological fields for July 2007. The monthly mean of absolute error is mostly < 30% with an average of 11% (auxiliary material[1]). The overall error of the top-down emissions over polluted areas is estimated at ∼50%. The uncertainty of the a priori inventory is ∼60% over the regions (section 3). *Wang et al.* [2007b] suggested that considering the contributions from non-surface sources (such as lightning and aircraft) as background NO$_2$ columns improves the top-down emission estimate. We follow the same approach here. The effect of lightning NO$_x$ on inversion is small. In a sensitivity study, we use OMI measurements only when lightning NO$_2$ fraction is < 10% of the simulated tropospheric columns, the resulting a posteriori emissions do not change.

[13] In the assimilated daily inversion, we use the same framework by *Martin et al.* [2003] outlined above. The inversion is applied daily using model results and OMI measurements to estimate the a posteriori emissions and errors. After the inversion, the updated emission inventory and its errors are used as the a priori in the model simulation in the next day. Therefore, both the emission and its error are updated at the grids with OMI measurements each day. The weekend/weekday variation is accounted for in the inversion. The weekend/weekday emission ratios are initially set to be 1 and iteratively estimated through the daily inversion of OMI NO$_2$ measurements by comparing weekend emissions with week-

days. The computed ratios are used for the following weekend emissions. The ratio is as low as 0.7 over some urban regions, but is negligible over most regions of East China. The overall impact of the emission ratio deviations from 1 on the a posteriori NO$_x$ emissions is small. The a posteriori emission convergence time scale is ∼10 days (auxiliary material). To further minimize the effect of single-day OMI measurements, we used the average of the a posteriori emissions (and their errors) of the last week as the a posteriori result of the assimilated inversion. More detailed description of the inversion procedure is provided in the auxiliary material. Since the computer resource needed in the inversion is small compared to the 3-D model simulation, assimilated inversion does not increase the computing resource need.

[14] We show here the difference between the a priori emissions and either monthly-mean or assimilated inversion results in case A (Figure 1a). The assimilated inversion leads to more significant adjustments than the monthly-mean inversion. The total a posteriori surface NO$_x$ emissions over east Asia are 11.2 and 11.0 Tg N/yr, respectively for monthly-mean and assimilated inversions, 3% and 5% less than the a priori total in case A (11.6 Tg N/yr). In case B (not shown), the total monthly-mean and assimilated a posteriori emissions are 9.8 and 10.6 Tg N/yr, respectively, 12% and 4% less than the a priori (11.1 Tg N/yr). The covariances (R^2 values) and root mean squared errors (RMSE) between simulated and OMI observed tropospheric NO$_2$ columns for July 2007 are listed in Table 1. The inversions increase the R^2 values and decrease the RMSE compared to the a priori emissions. The assimilated inversion yields better statistics (R^2: 0.92; RMSE: 0.56–0.58 × 10^{15} molcecules/cm^2) compared to the monthly-mean inversions (R^2: 0.78–0.82; RMSE: 0.81–0.91 × 10^{15} molecules/cm^2). We find similar improvements when

Table 1. Correlation Statistics Between OMI Retrieved and REAM Simulated Tropospheric NO$_2$ Columns With Different Surface NO$_x$ Emissions for July and August 2007

	A Priori				Monthly a Posteriori[a]				Assimilated a Posteriori[a]			
	Case A		Case B		Case A		Case B		Case A		Case B	
	Jul	Aug	Jul	Aug	Jul	Aug	Jul	Aug	Jul	Aug	Jul	Aug
R^2	0.61	0.54	0.53	0.48	0.82	0.81	0.78	0.76	0.93	0.90	0.92	0.90
RMSE (10^{15} molec/cm^2)	1.27	1.50	1.69	1.84	0.81	0.80	0.91	0.89	0.56	0.62	0.58	0.61

[a]The a posteriori emissions of NO$_x$ of July are used in the simulations for August.

applying these a posteriori emissions to a different month of August 2007 (Table 1).

[15] The spatial covariance between cases A and B improves to a R^2 value of 0.60 in the monthly-mean a posteriori emissions from 0.40 in the a priori emissions. In the assimilated inversions, the a posteriori emissions between the two cases are almost the same (R^2: 0.94), indicating that the assimilated inversion is insensitive to the a priori emissions unlike the monthly-mean inversion. In regions where a priori emissions are not known well, this is a significant advantage of the assimilated inversion method. The a posteriori emission uncertainties are reduced. The a posteriori error decreases until the emissions converge. 17% is estimated for the assimilated inversion compared to 60% and 36% for the a priori inventory and monthly-mean inversion, respectively. The uncertainty estimate for monthly inversion is an upper bound since we follow *Martin et al.* [2003] by assigning the daily retrieval error as the monthly-mean one.

4.3. Optimized Fossil-Fuel NO$_x$ Emission

[16] Since the assimilated a posteriori NO$_x$ emissions from two cases are almost the same, we use the assimilated a posteriori emissions in case A here. Partitioning between fossil fuel and soil emissions is not apparent from the column measurements. Since the change of total emissions is relatively small, we use the least-squares regression to linearly partition the a posteriori emissions based on the a priori fossil fuel and soil emissions, i.e., $E_{posteriori} = aE_{priori}^{fuel} + bE_{priori}^{soils}$ (more details in the auxiliary material). We obtain the a posteriori soil NO$_x$ emissions of 1.6 Tg N/yr for July, a factor of 2.4 higher than the a priori value of 0.68 Tg N/yr. It accounts for ∼14% of the total a posteriori emissions, significantly less than suggested by *Wang* [2007b] (auxiliary material).

[17] Subtracting the soil emissions, we obtain the a posteriori fossil fuel emissions (the data are available in the auxiliary material). Over the regions with significant fossil fuel emissions, such as East China, the a posteriori emissions are essentially from fossil fuel combustion. The total a posteriori fossil fuel NO$_x$ emission over east Asia is estimated as 9.5 Tg N/yr, 13% less than the a priori value of 10.9 Tg N/yr in case A. Table 2 lists the a priori and a posteriori total emissions over China, South Korea, Japan, and other countries in east Asia. Again the total emission change is relatively small. In both inventories, emissions from China account for ∼80% of the regional total.

[18] The most significant change from the a priori emissions is in the spatial distribution. The a posteriori fossil fuel NO$_x$ emissions and its spatial distribution changes from the a priori inventory are shown in Figure 2. Relative changes of 20–100% are found over the industrialized East China plains. Compared with the a posteriori results, the a priori inventory generally overestimates the emissions over the economically developed areas surrounding major urban centers and underestimates over the underdeveloped areas in East China. The bias likely reflects more stringent emission control policies and enforcements in urban regions and the presence of inefficient and unregulated local power and metallurgical plants in rural areas. A priori emissions from Shanxi, where coal production is prevalent, are underestimated throughout the province. A further study shows that the a posteriori emission distributions do not change if we expand the analysis period to other years (2005 and 2006) in summer.

5. Conclusions

[19] We develop a new daily assimilated inversion method to improve the top-down constraints of NO$_x$ emissions over east Asia based on OMI NO$_2$ measurements in July 2007. The iterative nature of the assimilated inversion accounts for the chemical feedbacks of NO$_x$ emission changes and reduces the dependence of the a posteriori emissions on the a priori emissions, resulting in significant improvements over the monthly-mean inversion result. The spatial covariance (R^2)

Table 2. A Priori and Assimilated a Posteriori Fossil Fuel NO$_x$ Emissions Over East Asia for 2007 (Tg N/yr)

	A Priori	Assimilated a Posteriori
China	8.48	7.48
South Korea	0.36	0.28
Japan	0.67	0.68
Other	1.40	1.03
Total	10.9	9.5
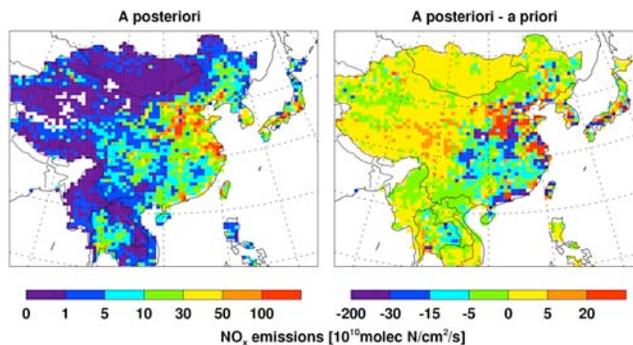
Figure 2. (left) Assimilated a posteriori fossil fuel NO$_x$ emissions over east Asia in case A, and (right) the corresponding changes in the a posteriori emissions from the a priori.

between observed and simulated NO_2 columns increases from 0.7–0.8 in monthly-mean inversion to 0.92; the RMSE is reduced by 30%. Similar improvements are found when these a posteriori emissions are applied to a different month. We find a relatively small contribution from soil emissions, ~1.6 Tg N/yr or ~14% in July. Annualized contribution will be even smaller because of the temperature dependence of soil emissions. The assimilated a posteriori NO_x emissions from fossil fuel combustion over east Asia are 9.5 Tg N/yr, 13% lower than the a priori value of 10.9 Tg N/yr in case A. While the total emission change is small (less than the uncertainty of 17% in the assimilated a posteriori inventory), significant spatial distribution changes are found, especially over East China. The a priori fossil fuel NO_x emission inventory tends to overestimate the emissions over the economically developed areas and underestimate over the underdeveloped areas in East China. While the dichotomy of a prior inventory bias may indicate an issue with the bottom-up statistics used to derive the inventory, it may also reflect in part fossil fuel NO_x emission reductions resulting from the urban-centric air quality controls and enforcements in China.

References

Benkovitz, C. M., M. T. Scholtz, J. Pacyna, L. Tarrasón, J. Dignon, E. C. Voldner, P. A. Spiro, J. A. Logan, and T. E. Graedel (1996), Global gridded inventories of anthropogenic emissions of sulfur and nitrogen, *J. Geophys. Res.*, *101*, 29,239–29,253.

Bey, I., D. J. Jacob, R. M. Yantosca, J. A. Logan, B. D. Field, A. M. Fiore, Q. Li, H. Y. Liu, L. J. Mickley, and M. G. Schultz (2001), Global modeling of tropospheric chemistry with assimilated meteorology: Model description and evaluation, *J. Geophys. Res.*, *106*, 23,073–23,095.

Boersma, K. F., et al. (2007), Near-real time retrieval of tropospheric NO_2 from OMI, *Atmos. Chem. Phys.*, *7*, 2103–2118.

Boersma, K. F., et al. (2008), Validation of OMI tropospheric NO_2 observation during INTEX-B and application to constrain NO_x emissions over the eastern United States and Mexico, *Atmos. Environ.*, *42*, 4480–4497.

Bucsela, E. J., E. A. Celarier, M. O. Wening, J. F. Gleason, J. P. Veefkind, K. F. Boersma, and E. J. Brinksma (2006), Algorithm for NO_2 vertical column retrieval from the Ozone Monitoring Instrument, *IEEE Trans. Geosci. Remote Sens.*, *44*, 1245–1258.

Bucsela, E. J., et al. (2008), Comparison of tropospheric NO_2 from in situ aircraft measurements with near-real-time and standard product data from OMI, *J. Geophys. Res.*, *113*, D16S31, doi:10.1029/2007JD008838.

Choi, Y., Y. Wang, T. Zeng, R. V. Martin, T. P. Kurosu, and K. Chance (2005), Evidence of lightning NO_x and convective transport of pollutants in satellite observations over North America, *Geophys. Res. Lett.*, *32*, L02805, doi:10.1029/2004GL021436.

Choi, Y., Y. Wang, T. Zeng, D. Cunnold, E.-S. Yang, R. Martin, K. Chance, V. Thouret, and E. Edgerton (2008a), Springtime transitions of NO_2, CO, and O_3 over North America: Model evaluation and analysis, *J. Geophys. Res.*, *113*, D20311, doi:10.1029/2007JD009632.

Choi, Y., Y. Wang, Q. Yang, D. Cunnold, T. Zeng, C. Shim, M. Luo, A. Eldering, E. Bucsela, and J. Gleason (2008b), Spring to summer northward migration of high O_3 over the western North Atlantic, *Geophys. Res. Lett.*, *35*, L04818, doi:10.1029/2007GL032276.

Granier, C., J. F. Lamarque, A. Mieville, J. F. Muller, J. Olivier, J. Orlando, J. Peters, G. Petron, G. Tyndall, and S. Wallens (2005), POET, a database of surface emissions of ozone precursors, http://www.aero.jussieu.fr/projet/ACCENT/POET.php, Atmos. Composition Change the Eur. Network of Excellence, Jussieu, France.

Guillas, S., J. Bao, Y. Choi, and Y. Wang (2008), Downscaling of chemical transport ozone forecasts over Atlanta, *Atmos. Environ.*, *42*, 1338–1348.

Jing, P., D. Cunnold, Y. Choi, and Y. Wang (2006), Summertime tropospheric ozone columns from Aura OMI/MLS measurements versus regional model results over the United States, *Geophys. Res. Lett.*, *33*, L17817, doi:10.1029/2006GL026473.

Kaufman, Y. J., C. O. Justice, L. P. Flynn, J. D. Kendall, E. M. Prins, L. Giglio, D. E. Ward, W. P. Menzel, and A. W. Setzer (1998), Potential global fire monitoring from EOS-MODIS, *J. Geophys. Res.*, *103*, 32,215–32,238.

Lamsal, L. N., R. V. Martin, A. van Donkelaar, M. Steinbacher, E. A. Celarier, E. Bucsela, E. J. Dunlea, and J. P. Pinto (2008), Ground-level nitrogen dioxide concentrations inferred from the satellite-borne Ozone Monitoring Instrument, *J. Geophys. Res.*, *113*, D16308, doi:10.1029/2007JD009235.

Ma, J., A. Richter, J. P. Burrows, H. Hub, and J. A. van Aardenne (2006), Comparison of model-simulated tropospheric NO_2 over China with GOME-satellite data, *Atmos. Environ.*, *40*, 593–604.

Martin, R. V., D. J. Jacob, K. Chance, T. P. Kurosu, P. I. Palmer, and M. J. Evans (2003), Global inventory of nitrogen oxide emissions constrained by space-based observations of NO_2 columns, *J. Geophys. Res.*, *108*(D17), 4537, doi:10.1029/2003JD003453.

Martin, R. V., C. E. Sioris, K. Chance, T. B. Ryerson, T. H. Bertram, P. J. Wooldridge, R. C. Cohen, J. A. Neuman, A. Swanson, and F. M. Flocke (2006), Evaluation of space-based constraints on global nitrogen oxide emissions with regional aircraft measurements over and downwind of eastern North America, *J. Geophys. Res.*, *111*, D15308, doi:10.1029/2005JD006680.

Stavrakou, T., J.-F. Müller, K. F. Boersma, I. De Smedt, and R. J. van der A (2008), Assessing the distribution and growth rates of NO_x emission sources by inverting a 10-year record of NO_2 satellite columns, *Geophys. Res. Lett.*, *35*, L10801, doi:10.1029/2008GL033521.

Streets, D. G., et al. (2003), An inventory of gaseous and primary aerosol emissions in Asia in the year 2000, *J. Geophys. Res.*, *108*(D21), 8809, doi:10.1029/2002JD003093.

Wang, Y., D. J. Jacob, and J. A. Logan (1998), Global simulation of tropospheric O_3-NO_x-hydrocarbon chemistry: 3. Origin of tropospheric ozone and effects of nonmethane hydrocarbons, *J. Geophys. Res.*, *103*, 10,757–10,767.

Wang, Y., Y. Choi, T. Zeng, B. Ridley, N. Blake, D. Blake, and F. Flocke (2006), Late-spring increase of trans-Pacific pollution transport in the upper troposphere, *Geophys. Res. Lett.*, *33*, L01811, doi:10.1029/2005GL024975.

Wang, Y. H., Y. Choi, T. Zeng, D. Davis, M. Buhr, L. Huey, and W. Neff (2007a), Assessing the photochemical impact of snow NO_x emissions over Antarctica during ANTCI 2003, *Atmos. Environ.*, *41*, 3944–3958.

Wang, Y., M. B. McElroy, R. V. Martin, D. G. Streets, Q. Zhang, and T.-M. Fu (2007b), Seasonal variability of NO_x emissions over east China constrained by satellite observations: Implications for combustion and microbial sources, *J. Geophys. Res.*, *112*, D06301, doi:10.1029/2006JD007538.

Yienger, J. J., and H. Levy II (1995), Empirical model of global soil-biogenic NO_x emissions, *J. Geophys. Res.*, *100*, 11,447–11,464.

Zeng, T., Y. Wang, K. Chance, E. V. Browell, B. A. Ridley, and E. L. Atlas (2003), Widespread persistent near-surface ozone depletion at northern high latitudes in spring, *Geophys. Res. Lett.*, *30*(24), 2298, doi:10.1029/2003GL018587.

Zeng, T., Y. Wang, K. Chance, N. Blake, D. Blake, and B. Ridley (2006), Halogen-driven low-altitude O_3 and hydrocarbon losses in spring at northern high latitudes, *J. Geophys. Res.*, *111*, D17313, doi:10.1029/2005JD006706.

Zhang, Q., et al. (2007), NO_x emission trends for China, 1995–2004: The view from the ground and the view from space, *J. Geophys. Res.*, *112*, D22306, doi:10.1029/2007JD008684.

Zhao, C., Y. Wang, Y. Choi, and T. Zeng (2008), Impact of convective transport and lightning NO_x production over North America: Dependence on cumulus parameterizations, *Atmos. Chem. Phys. Discuss.*, *9*, 2289–2317.

————————————
Y. Wang and C. Zhao, School of Earth and Atmospheric Science, Georgia Institute of Technology, 311 Ferst Drive, Atlanta, GA 30332, USA. (chun.zhao@eas.gatech.edu)